HHS Public Access

Author manuscript

J Thromb Haemost. Author manuscript; available in PMC 2017 December 01.

Published in final edited form as:

J Thromb Haemost. 2016 December ; 14(12): 2509–2523. doi:10.1111/jth.13538.

S2′-subsite variations between human and mouse enzymes (plasmin, FXIa, kallikrein) elucidate differences in inhibition by TFPI-2 $KD1_{WT}$-V_T, $KD1_{L17R}$-K_T and aprotinin

K. Vadivel[*], **Y. Kumar**[*], **G. I. Ogueli**[*], **S. M. Ponnuraj**[*], **P. Wongkongkathep**[†], **J. A. Loo**[†,‡], **M. S. Bajaj**[§], and **S. P. Bajaj**[*,‡]

[*]Department of Orthopaedic Surgery, University of California, Los Angeles, CA

[†]Department of Chemistry and Biochemistry, UCLA, Los Angeles, CA

[‡]Molecular Biology Institute, University of California, Los Angeles, CA

[§]Department of Medicine, Division of Pulmonology and Critical Care, University of California, Los Angeles, CA, USA

Summary

Background—Using TFPI-2 Kunitz domain1 (KD1), we obtained a bifunctional antifibrinolytic molecule ($KD1_{L17R}$-K_T) with C-terminal lysine (kringle domain binding) and P2′-residue arginine (improved specificity towards plasmin). $KD1_{L17R}$-K_T strongly inhibited human plasmin (hPm), with no inhibition of human kallikrein (hKLK) or factor XIa (hXIa). Furthermore, $KD1_{L17R}$-K_T reduced blood loss comparable to aprotinin in a mouse liver-laceration model of organ hemorrhage. However, effectiveness of these antifibrinolytic agents in a model of hemorrhage mimicking extremity trauma and their inhibition efficiencies for mouse enzymes (mPm, mKLK or mXIa) remain to be determined.

Objective—Determine potential differences in inhibition constants of various antifibrinolytic agents against mouse and human enzymes and test their effectiveness in a modified mouse tail-amputation hemorrhage model.

Methods/Results—Unexpectedly, mXIa was inhibited with ~17-fold increased affinity by aprotinin (K_i ~20 nM) and with measurable affinity for $KD1_{L17R}$-K_T (K_i ~3 μM); in contrast, $KD1_{WT}$-V_T inhibited hXIa or mXIa with similar affinity. Compared to hPm, mPm had ~3-fold reduced affinity, whereas species specificity for hKLK and mKLK were comparable for each inhibitor. S2′-subsite variations largely accounted for the observed differences. $KD1_{L17R}$-K_T and

Correspondence to: S. Paul Bajaj, 615 Charles E. Young Drive, Los Angeles, California 90095, USA, Tel: 01-310-825-5622, Fax: 01-310-825-5972, pbajaj@mednet.ucla.edu.

Addendum

K. Vadivel performed enzyme inhibition, molecular modeling and structural analysis, and wrote the manuscript. Y. Kumar performed enzyme inhibition, fibrinolysis and animal experiments. G.I. Ogueli expressed $KD1_{WT}$-V_T and $KD1_{L17R}$-K_T proteins. S.M. Ponnuraj processed mouse blood samples and performed D-dimer assays. P. Wongkongkathep and J.A. Loo performed mass spectrometry experiments. M.S. Bajaj and S.P. Bajaj conceived, designed, analyzed and interpreted the data, and wrote the manuscript.

Disclosure of conflict of interests

S.P. Bajaj has patents issued and pending on the $KD1_{L17R}$-K_T and related molecules. The view and conclusions drawn are the sole responsibility of the authors.

aprotinin were more effective than $KD1_{WT}$-V_T or tranexamic acid in inhibiting tPA-induced mouse plasma clot lysis. Further, $KD1_{L17R}$-K_T was more effective than $KD1_{WT}$-V_T and was comparable to aprotinin and tranexamic acid in reducing blood loss and D-dimer levels in the mouse tail-amputation model.

Conclusions—Inhibitor potencies differ between antifibrinolytic agents against human and mouse enzymes. $KD1_{L17R}$-K_T is effective in reducing blood loss in a tail-amputation model that mimics extremity injury in trauma.

Keywords

Antifibrinolytic agents; Aprotinin; Fibrinolysis; TFPI-2; Tranexamic acid

Introduction

Trauma or major surgery results in severe tissue damage and rupture of both the small and large vessels in the injured area. Tissue damage leads to local platelet adhesion and aggregation with formation of the primary hemostatic plug. The platelet plug is then strengthened and stabilized by a fibrin network generated through extrinsic and intrinsic coagulation. As the damaged vessels heal, the fibrin clot is lysed to ensure normal blood flow. The breakdown of the clot, fibrinolysis, is due to plasmin (Pm) generated from plasminogen by tissue plasminogen activator (tPA) released from the damaged endothelium [1–3]. However, severe trauma and major surgery frequently evoke hyperfibrinolysis resulting in massive hemorrhage necessitating the use of increased blood products [4–6], which are associated with a high risk of adverse clinical outcomes. These include morbidity and mortality related to transfusion-associated acute lung injury [7,8] as well as transfusion-related immunomodulation and transfusion-associated circulatory overload [8].

Antifibrinolytic agents are useful in preventing blood loss during trauma and major surgical procedures such as cardiopulmonary bypass surgery as well as in reducing the risk of surgical revision due to post-operative bleeding [9,10]. Approximately 4–6% of these patients (~25,000 patients/year in the Unites States) need surgical revision due to bleeding following cardiac surgery [10]. Antifibrinolytic agents when used prophylactically can significantly reduce blood loss and the need for surgical revision as well as the intraoperative and postoperative requirement for allogeneic blood transfusions [9–11]. After the withdrawal of aprotinin (Trasylol®, bovine pancreatic trypsin inhibitor, BPTI) from the world market in year 2008 following the BART study [12], tranexamic acid (TXA) and ε-amino caproic acid (EACA), are the two antifibirinolytics currently in use. However, emerging reports of observational clinical trials (Table S1) reveal that upsurge in the use of TXA [10,12–20] and EACA [10,12,18–22] in patients undergoing cardiac surgery is associated with seizures (1.3–10% TXA; 3.3% EACA) and renal dysfunction (1.5–20% TXA; 12.9–40% EACA) leading to an increase in hospital stay and mortality rate (2.5–7.5% TXA; 2.4–4.0% EACA). Although not in every study [23–27], seizures have also been observed with TXA or EACA in mice [28,29], rats [30,31], and cats [32,33], whereas renal injury has been observed with aprotinin in mice [34] and rats [35]. These observations highlight a need for development of an alternate antifibirnolytic agent that prevents blood loss without the serious adverse effects during surgery and trauma.

TXA and EACA bind to the kringle-lysine binding sites (LBS) of tPA and plasminogen and thereby prevent their binding to the exposed C-terminal lysine residues of fibrin; as a result activation of plasminogen to Pm and fibrinolysis at the clot site is impeded [36,37]. Since currently available active site inhibitors of plasmin or the LBS inhibitors of fibrinolysis are associated with adverse effects, a concerted effort is directed towards development of new safer inhibitors of fibrinolysis [38–47]. In this context, we used Kunitz domain1 (KD1) of human tissue factor pathway inhibitor type-2 (TFPI-2) to obtain a specific inhibitor ($KD1_{L17R}$-K_T) of human Pm (hPm) by targeting the S2′-pocket. Further, $KD1_{L17R}$-K_T also binds to the LBS of tPA or plasminogen with ~300 nM K_d [29]. Unlike KD1 wild-type molecule with C-terminal valine ($KD1_{WT}$-V_T) or aprotinin [34], $KD1_{L17R}$-K_T (or $KD1_{L17R}$-V_T) does not inhibit human factor XIa (hXIa) or plasma kallikrein (hKLK). Further, similar to aprotinin and the lysine analog TXA or EACA, $KD1_{L17R}$-K_T is effective in reducing blood loss in the mouse liver-laceration model [29]. Importantly, it does not appear to cause seizures in mice [29] and renal injury in mice [34] or rats [35]. Although, $KD1_{L17R}$-K_T is effective in reducing blood loss in the liver-laceration model of organ trauma, its antifibrinolytic potential in hemorrhage from extremity trauma has not been evaluated. Moreover, inhibition by $KD1_{WT}$-V_T/$KD1_{L17R}$-K_T or aprotinin of mouse enzymes (mPm, mIXa, mKLK), the animal used for studies, is not known.

Here, we examined reduction of blood loss by $KD1_{L17R}$-K_T in a modified mouse tail-amputation model, which resembles hemorrhage from extremity trauma concerning tissue, bone and large vessel damage. In our model, tail is amputated at 4 cm vs 0.5 cm in previous reports for testing systemic and topical antifibrinolytic agents [48,49]. Since animal studies are performed in mice, we examined specificity of human $KD1_{WT}$-V_T, $KD1_{L17R}$-K_T or bovine aprotinin for mouse enzymes (mPm, mXIa and mKLK). Further, aprotinin strongly inhibits bovine trypsin, a coagulation-type protease; thus, we examined inhibition of trypsin by $KD1_{L17R}$-K_T. We present these findings here and provide rationale for the observed differences between human and mouse enzymes by structural models.

Materials and methods

Materials

Citrated mouse plasma was from Innovative Research (Novi, MI). Aprotinin was from ZymoGenetics (Seattle, WA) and tissue plasminogen activator (tPA) was from Genentech (South San Francisco, CA). Pm substrate S-2251 (H-D-Val-Leu-Lys-*p*-nitroanilide), and KLK and Factor XIa substrate S-2366 (pyroGlu-Pro-Arg-*p*-nitroanilide) were from Diapharma Inc. Asserachrom D-Di ELISA kit was from Diagnostica Stago, Inc (Parsippany, NJ). Human α-thrombin (IIa), specific activity ~4493 U/mg (fibrinogen clotting assay), and mPm were from Haematologic Technologies Inc. Human alpha-XIIa was from Enzyme Research Laboratories. mKLK and mXI were from R&D Systems Inc. mXI (100 μg/ml) was activated at 37 °C by factor alpha-XIIa using a 1:20 molar ratio in 50 mM Tris-HCl, pH 7.5 containing 100 mM NaCl (TBS) and 2 mM $CaCl_2$. One μL aliquots were withdrawn at different times, diluted to 100 μL in TBS containing 0.1 mg/ml bovine serum albumin (TBS/BSA, pH 7.5) and 2 mM $CaCl_2$. The formation of mXIa was measured by hydrolysis of synthetic chromogenic substrate S2366 (330 μM). Activation was complete in 4 hrs as

measured by mXIa hydrolytic activity and SDS-PAGE [50]. Under reduced conditions, mXI (2 μg) migrated as a single band with MW of ~80,000 Da and mXIa (2 μg) migrated as two bands with MWs of ~45,000 Da and ~37,000 Da. The mXIa was kept on ice and used within 24 hrs.

Expression, purification and characterization of $KD1_{WT}$-V_T and $KD1_{L17R}$-K_T

The procedures to obtain $KD1_{WT}$-V_T and $KD1_{L17R}$-K_T have been described earlier [29,34,51,52]. Briefly, the 73 amino acid $KD1_{WT}$-V_T and $KD1_{L17R}$-V_T were over-expressed as amino-terminal His_6-tagged fusion proteins in *E. coli* strain BL21(DE3) pLysS using the T7 promoter system. To obtain $KD1_{L17R}$ with a C-terminal lysine ($KD1_{L17R}$-K_T), $KD1_{L17R}$-V_T was incubated with IIa at a 1:50 enzyme/substrate ratio for 24 hrs at 37°C [29]. The His_6-tag free proteins were purified using Superdex 200 gel filtration chromatography equilibrated with TBS as outlined [29,34,51,52]. The purified $KD1_{WT}$-V_T and $KD1_{L17R}$-K_T were checked for purity (SDS-PAGE) and characterized using N-terminal sequencing and mass spectrometry prior to performing biochemical and animal studies.

Protease inhibition assay

Reactions were carried out in TBS/BSA/2 mM Ca^{2+}, pH 7.5. Each enzyme (mPm, mKLK and mXIa) was incubated with various concentrations of $KD1_{L17R}$-K_T, $KD1_{WT}$-V_T, aprotinin or trypsin for 1 hr at RT in a 96-well microtitration plate (total volume 100 μL). Synthetic substrate (5 μL) specific for each enzyme was then added (final concentration, 1 K_M) and residual amidolytic activity was measured in a Molecular Devices V_{max} kinetic microplate reader. The inhibition constants, K_i^*, were determined using the nonlinear regression data analysis program GraFit. Data were analyzed with an equation for a tight-binding inhibitor (Equation 1) where v_i and v_0 are the inhibited and uninhibited rates, respectively, and $[I]_0$ and $[E]_0$ are the total concentrations of inhibitor and enzyme, respectively [53,54].

$$v_i = v_0 \frac{\left((K_i^* + [I]_0 + [E]_0)^2 - 4[I]_0[E]_0 \right)^{1/2} - (K_i^* + [I]_0 - [E]_0) \right)}{2[E]_0} \quad \text{Equation 1}$$

K_i values were obtained by correcting for the effect of substrate according to Beith [53], using Equation 2, where [*S*] is substrate concentration and K_M is specific for each enzyme.

$$K_i = K_i^* / (1 + [S]/K_M) \quad \text{Equation 2}$$

Fibrinolysis (clot lysis) assay

Ten μL of each test compound or saline control was added to 240 μL of mouse plasma; 225 μL of this mixture was then added to 25 μL IIa and tPA in TBS/BSA containing 25 mM $CaCl_2$. The final concentration of IIa was 0.15 μg/ml, and of tPA was 1 μg/ml. Clot

formation and lysis were monitored (OD_{405}) with a Molecular Devices microplate reader (SPECTRAmax 190) as described earlier [29,34].

Mouse tail-amputation model

A protocol using the tail-amputation mouse model was approved by the UCLA Chancellor's animal research committee. In this model, tail is amputated at 4 cm from the tip that involves cutting the bone, which we hypothesize will increase local activation of the fibrinolytic system due to enhanced vascular and tissue trauma. Five groups of C57BL/6 mice (~20 gm in weight) of both sexes were used for saline control, positive controls (aprotinin and TXA) and experimental drugs ($KD1_{L17R}$-K_T and $KD1_{WT}$-V_T). Animals were fed standard rodent chow and water, and housed in a vivarium room maintained at 20–24 °C and 12-h light-dark cycles. Dosage of aprotinin was comparable to that used in humans, i.e. 4 μg/g adjusted for mouse weight [55]. A calculated blood level (based on 10 ml volume of distribution) achieved by this dose was ~8 μg/ml (~1 μM). Since $KD1_{WT}$-V_T and $KD1_{L17R}$-K_T are homologs of aprotinin, a similar dose of each KD1 variant was used.

Variable concentrations of TXA have been used in different animal models [23–27]. We used 10 μg/g adjusted for mouse weight (calculated TXA blood level ~20 μg/ml or ~125 μM) based upon the dose used in one regimen to prevent blood loss in a major surgical procedure [55]. Such dose has also been reported to be adequate to prevent systemic fibrinolysis and local fibrinolytic bleedings [56].

All animals were run in a single big randomized experiment and all compounds including saline were tested during each batch. Anesthesia was induced using 5% isoflurane via nosecone. Following induction of anesthesia, mice were placed on a heating pad to maintain rectal temperature at 37 °C. Drugs were injected via tail vein in 100 μL of sterile, balanced salt solution. Care was taken to avoid extravasation and to avoid injecting the drug close to the site of amputation so as to minimize the potential local effect of any extravasated drug. After allowing two minutes for circulation, tail was amputated at 4 cm from the tip using a sharp, sterile, #11 scalpel blade. Anesthesia was maintained with 2% isoflurane via nosecone during the entire experiment. Blood was allowed to flow freely into preweighed eppendorf tubes. Care was taken not to disturb the bleeding tip. Total time of observation was 1 hour, based on the literature and the preliminary experiments during which normal controls demonstrated any significant recurrence of bleeding, potentially from alternate constriction and dilation of the central artery [57].

Bleeding time varied between 8 to 13 min with minimal recurrent bleeding except in the saline group that lasted occasionally up to 30 min. The plasma half-life of TXA in humans, rats and dogs is ~120 min [58]. The half-life of the two KD1 variant homologs (aprotinin and Ecallantide) is also ~120 min [59,60] in humans, whereas of aprotinin in mice, rats or dogs is ~70 min [61]. The half-life of each KD1 variant could also be similar to aprotinin/Ecallantide. Based upon these data, adequate concentration of each drug is presumed to exist up to the cessation time of bleeding. No deaths were observed in any of the five groups. At the end of the experiment, citrated blood was obtained from the lateral saphenous vein for D-dimer assay by venipuncture. After removing the RBC, mouse plasma was obtained by centrifugation for 15 min at 1500g, 4 °C. The data were combined after the completion of all

experiments and analyzed. Since all animals were similar in weight and treated alike, potential temporal effects were minimized and no correction was applied. Primary outcome was total blood loss and plasma D-dimer levels.

Statistical methods

We compared mean total blood loss across all five treatment groups using factorial one-way analysis of variance (ANOVA). The *p*-values for comparing any two means were computed using post-hoc tests and adjusted for multiple comparisons using Tukey's adjustment. For the D-dimer data, Levene's F-test revealed that the homogeneity of variance was not met. As such, the Welch's F-test was used and Games-Howell post-hoc procedure was conducted to determine which pairs of the five mean D-dimer levels differ significantly. All statistical analysis was performed using SPSS V23 (IBM Corp., Armonk, NY, USA).

Molecular modeling

The MODELLER program [62] was employed to model the protease domains of mPm, mXIa and mKLK using PDB entries 1BUI (hPm), 1ZJD (hXIa) and 2ANY (hKLK) as templates [63]. The modeled structures were energy minimized with backbone restraints using CHARMM [64] and were free of Ramachandran outliers. The complexes of $KD1_{WT}$-V_T, $KD1_{L17R}$-K_T and BPTI with mPm, mXIa and mKLK were modeled as described earlier [34,51,52] and energy minimized with backbone restraints using CHARMM prior to analysis. The trypsin-BPTI complex (2PTC) and trypsin-$KD1_{WT}$-V_T complex (1ZR0) were used for structural analysis. The electrostatic potentials were calculated using ABPS module implemented in PyMOL [65,66].

Results and Discussion

Molecular characterization of $KD1_{WT}$-V_T and $KD1_{L17R}$-K_T molecules

The $KD1_{WT}$-V_T preparation is homogeneous and has C-terminal Val73 as determined by SDS-PAGE, mass spectrometry and N-terminal sequence analysis (Fig. 1A). Isolated $KD1_{L17R}$-K_T has C-terminal Lys72 (~92%) with minor proteolysis at the N-terminus between residues Ala3↓Gln4, Gln4↓Glu5, and Thr7↓Gly8 (Fig. 1B). Since Kunitz domain starts at residue 10 (number 1 in BPTI, Fig. 1), the inhibitory domain of $KD1_{L17R}$-K_T is intact and only ~8% of the preparation has C-terminal Val73 that is devoid of binding to the kringle domains of tPA and plasminogen. These data indicate that $KD1_{L17R}$-K_T preparation is suitable for use as a dual reactivity antifibrinolytic agent, which can inhibit the active site of Pm as well as bind to the kringle domains of tPA and plasminogen.

Inhibitory properties of $KD1_{WT}$-V_T, $KD1_{L17R}$-K_T and aprotinin (BPTI) against mPm, mXIa, mKLK and bovine trypsin

$KD1_{L17R}$-K_T inhibits hPm effectively without inhibiting hXIa and hKLK [34]. Since potency of $KD1_{L17R}$-K_T is tested in a mouse bleeding model, we determined its inhibitory proficiency against mPm, mXIa and mKLK, and compared such data obtained with $KD1_{WT}$-V_T and aprotinin. Further, S2′-pocket of trypsin lacks acidic residues, which is a hallmark of Pm [34]; however, aprotinin (P2′ Arg17) inhibits trypsin with pM affinity [67]. We sought an explanation for this observation and examined whether $KD1_{L17R}$-K_T also inhibits trypsin.

Inhibition of mPm by $KD1_{WT}$-V_T, $KD1_{L17R}$-K_T and aprotinin—mPm was inhibited by $KD1_{WT}$-V_T with ~18 nM K_i, by KD_{L17R}-K_T with ~4 nM K_i, and by aprotinin with ~1.5 nM K_i (Fig. 2A and Table 1). Thus, as compared to hPm, affinity of each inhibitor is reduced by ~3 to 4-fold for mPm. To understand these uniform differences in affinity of each inhibitor for mPm versus hPm, we obtained molecular models of the protease domains of hPm and mPm complexed with each inhibitor. Although, protease domains of hPm and mPm share ~83% sequence identity [68,69], the notable difference between the S2′-pocket of these two proteases is the presence of Met39 in hPm versus Gln39 in mPm. This is shown in Fig. 3A and Fig. 3B. In hPm, Leu17 of $KD1_{WT}$-V_T or Arg17 side chain hydrocarbons of $KD1_{L17R}$-K_T or BPTI are involved in hydrophobic contacts with Met39; however, such interactions are not possible in mPm due to the presence of Gln39 instead of Met39 (Fig. 3A and 3B). Further, Glu73 and Glu143 of hPm/mPm make salt-bridges with P2′ Arg17 of $KD1_{L17R}$-K_T or BPTI; such interactions are not possible for $KD1_{WT}$-V_T. As compared to $KD1_{WT}$-V_T, these additional interactions provide a reasonable explanation for the higher affinity of $KD1_{L17R}$-K_T or BPTI for hPm/mPm.

Inhibition of bovine trypsin by $KD1_{WT}$-V_T, $KD1_{L17R}$-K_T and aprotinin—Trypsin was inhibited by $KD1_{WT}$-V_T with ~17 nM K_i, by KD_{L17R}-K_T with ~7 nM K_i, and by aprotinin with ~0.07 nM K_i (Fig. 2B and Table 1). These data are in agreement with a K_i of ~13 nM for $KD1_{WT}$-V_T [51] and a very strong inhibition of trypsin by aprotinin [70]. Similar to the coagulation proteases [34], trypsin has a hydrophobic S2′-pocket that is devoid of acidic residues [52,70]. However, multiple sequence alignment of trypsin with coagulation proteases and plasmin reveal that Tyr39 and Tyr151 are unique to trypsin and are situated at the entrance of the S2′-pocket (Fig. 3C). Further, examination of the X-ray structures of trypsin in complex with $KD1_{WT}$-V_T [52] or aprotinin [70] reveal overall similar interactions except encompassing the S2′-pocket and the 90-loop. As shown in Fig. 3C, the P2′ Leu17 of $KD1_{WT}$-V_T makes hydrophobic contacts with Tyr39 and Tyr151 of trypsin [52]. The P2′ Arg17 of aprotinin makes a hydrogen bond with the main chain carbonyl of His40 as well as π-interactions with the phenyl ring of Tyr151 [70]. Moreover, as experimentally observed with aprotinin [70], P2′ Arg17 of $KD1_{L17R}$-K_T makes similar interactions with His40/Tyr151 of trypsin (Fig. 3C).

Additionally, Arg39 of BPTI is involved in hydrogen bond interactions with the main chain carbonyls of Asn97 and Thr98 in the 90-loop of trypsin [70]. As compared to trypsin, the 90-loop in hPm/mPm has four-residue deletion, which prevents such interactions between aprotinin and Pm (Fig. 3C). These differences could be a reason for stronger inhibition of trypsin versus hPm/mPm by aprotinin (Table 2). Interestingly, residue 39 is Glu in $KD1_{WT}$-V_T or $KD1_{L17R}$-K_T, which precludes its interactions involving the 90-loop of trypsin (or hPm/mPm). Thus, existence of interactions involving the 90-loop could explain the difference in affinity of aprotinin versus $KD1_{WT}V_T$ or $KD1_{L17R}$-K_T for trypsin.

Inhibition of mXIa by $KD1_{WT}$-V_T, $KD1_{L17R}$-K_T and aprotinin—$KD1_{WT}$-V_T inhibits mXIa and hXIa with similar affinity with K_i ~20 nM (Fig. 2C and Table 1). Although protease domains of hXIa and mXIa share ~78% sequence identity [71,72], the 39-loop in mXIa has a 3-residue deletion including Arg39D present in the S2′-pocket of hXIa.

However, P2′ Leu17 of $KD1_{WT}$-V_T is suitably placed in the S2′-pocket of mXIa (Fig. 4A) or hXIa [34] without interference from Arg39D. In contrast, $KD1_{L17R}$-K_T inhibits mXIa with K_i ~3 μM as compared to no inhibition observed upto 10 μM for hXIa (Fig. 2C and Table 1). A plausible explanation for this observation is the unfavorable interaction between Arg39D of hXIa and P2′ Arg17 of $KD1_{L17R}$-K_T and the absence of Arg39D in mXIa (Fig. 4B). Consequently, $KD1_{WT}$-V_T illustrates no difference in inhibition mXIa or hXIa, whereas $KD1_{L17R}$-K_T inhibits mXIa weakly.

Strikingly, aprotinin inhibits mXIa with K_i ~20 nM as compared to K_i ~350 nM for hXIa (Fig. 2C and Table 1). Similar to $KD1_{L17R}$-K_T, P2′ Arg17 of aprotinin is unfavorable to interact with Arg39D of hXIa; however, absence of Arg39D in mXIa abrogates this unfavorable interaction. Further, Arg39 of aprotinin interacts via salt-bridge with Glu98 and Glu217 of hXIa/mXIa, and these interactions are not possible for $KD1_{WT}$-V_T or $KD1_{L17R}$-K_T (Fig. 4C). Thus, as compared to hXIa, a ~17-fold increase in inhibition potential of aprotinin for mXIa primarily stems from the absence of unfavorable interactions between P2′ Arg17 and the S2′-pocket.

Inhibition of mKLK by $KD1_{WT}$-V_T, $KD1_{L17R}$-K_T and aprotinin—No significant differences were observed for inhibition of mKLK or hKLK by $KD1_{WT}$-V_T, $KD1_{L17R}$-K_T and aprotinin (Fig. 2D and Table 1). Although the protease domain of hKLK has Arg39 [73] instead of Thr in mKLK [74], P2′ Leu17 of $KD1_{WT}$-V_T is optimally placed in the S2′-pocket of either enzyme (Fig. 5A). The P2′ Arg17 of $KD1_{L17R}$-K_T or aprotinin is unfavorable to interact with Arg39 of hKLK (Fig. 5B), whereas it is not involved in any interaction with the S2′-pocket of mKLK. Note that unlike mXIa, the 39-loops of mKLK and hKLK have the same number of amino acids. Further, Arg39 and Tyr10 of aprotinin interact with Glu217 of hKLK/mKLK, and such interactions are not possible for $KD1_{L17R}$-K_T (or $KD1_{WT}$-V_T) (Fig. 5C). Thus, the presence of additional interactions allow aprotinin to inhibit hKLK/mKLK and their absence make $KD1_{L17R}$-K_T a non-inhibitor of hKLK/mKLK.

Fibrinolysis assay

Fibrinolysis data are presented in Fig. 6A–D. Addition of IIa to mouse plasma results in an increase in OD_{405} reflective of a stable clot formation (curve 1); however, simultaneous addition of tPA results in a biphasic curve with an initial increase in OD_{405} (fibrin formation), which is followed by a rapid decrease associated with the fibrinolytic activity (curve 2) induced by Pm that is formed by the action of tPA on plasminogen. The data presented in Fig. 6A–D reveal that similar to the human system [34], antifibrinolytic agents inhibit mouse plasma clot fibrinolysis in a dose dependent manner. Complete inhibition of fibrinolysis in this kinetic assay was achieved at ~20 μM for $KD1_{WT}$-V_T, at ~2 μM for $KD1_{L17R}$-K_T, at ~4 μM for aprotinin and at ~500 μM for TXA. Although aprotinin inhibits mPm with higher affinity than $KD1_{L17R}$-K_T (Fig. 2), the inhibition efficiency of each in preventing fibrinolysis is comparable (Fig. 6). These results indicate that the $KD1_{L17R}$-K_T prevents clot lysis by a dual mechanism especially at concentrations ≥1 μM; one, by inhibiting active site of plasmin and two, by inhibiting generation of plasmin at the clot site [29].

Blood loss and D-dimer levels in mouse tail-amputation model

Next, we studied the effect of $KD1_{L17R}$-K_T on blood loss and plasma D-dimer levels in the mouse tail-amputation model. The effects of all four antifibrinolytics on blood loss are depicted in Fig. 7A. There is a significant difference in the mean blood loss between groups as determined by one-way ANOVA ($F(4,45)=12.88$, $p=0.001$). A Tukey post-hoc test revealed that compared to saline, the mean blood loss was significantly lower for each antifibrinolytic group. Compared to saline, the mean blood loss was reduced by 190 mg for $KD1_{L17R}$-K_T (95% CI, 104–275; $p=0.001$), 176 mg for aprotinin (95% CI, 90–261; $p=0.001$), 112 mg for TXA (95% CI, 26–197; $p=0.005$), and 87 for $KD1_{WT}$-V_T (95% CI, 15–172; $p=0.044$). Further, as compared to $KD1_{WT}$-V_T, the mean blood loss was significantly reduced for $KD1_{L17R}$-K_T (95% CI, 17–188, $p=0.011$) or BPTI (95% CI, 4–175, $p=0.037$). However, differences in the mean blood loss reduction between $KD1_{L17R}$-K_T and aprotinin (95% CI, -71–99, $p=0.991$) as well as between $KD1_{L17R}$-K_T and TXA (95% CI, -7–162, $p=0.092$) or $KD1_{L17R}$-V_T and TXA (95% CI, -110–60, $p=0.917$) were statistically not significant. Notably, three of the ten animals treated with TXA depicted generalized seizures shortly after injection of the drug. The nature of the seizures were similar to those observed previously with EACA [29]. Further, $KD1_{L17R}$-K_T at the dose tested is comparable to TXA or aprotinin in minimizing the blood loss without observable seizures or renal injury [29,34,35].

All four antifibrinolytics also reduced plasma D-dimer levels (Fig. 7B). Compared to saline, the mean plasma D-dimer levels were reduced by 65 ng/ml for $KD1_{L17R}$-K_T (95% CI, 18–113, $p=0.008$), 60 ng/ml for aprotinin (95% CI, 11–108, $p=0.015$) and 55 ng/ml for TXA (95% CI, 6–105, $p=0.026$). Although the mean D-Dimer levels were reduced by 45 ng/ml for $KD1_{WT}$-V_T, it was statistically not significant (95% CI, -5–95, $p=0.091$) from saline. Importantly, these data indicate that the fibrinolytic system is activated in this model and $KD1_{L17R}$-K_T is comparable to aprotinin or TXA in inhibiting Pm-induced fibrinolysis.

Aprotinin is more potent (~3-fold) inhibitor of mPm than $KD1_{L17R}$-K_T; however, reduction in blood loss by both inhibitors is similar in the mouse liver-laceration [34] or the tail-amputation model. An explanation for this observation could be that aprotinin also attenuates intrinsic clotting by inhibiting mXIa (K_I~20 nM) and mKLK (K_i~10 nM), whereas inhibition of these enzymes by $KD1_{L17R}$-K_T is negligible (Table 1). Further, $KD1_{L17R}$-K_T could also inhibit fibrinolysis by impeding generation of Pm by tPA. It is also worth noting that two Pm inhibitors (Ecallantide and MDCO-2010), which inhibit KLK were unsuccessful in phase-3 clinical trials [42,44].

Conclusions

Employing enzyme assays and *in silico* modeling coupled with the existing crystallographic data [52,70], we provide structural explanations for strong inhibition of mXIa and mKLK by aprotinin and for negligible inhibition by $KD1_{L17R}$-K_T. Structural basis are also provided for inhibition of bovine trypsin by aprotinin and $KD1_{L17R}$-K_T despite the presence of P2′-Arg residue in these inhibitors. The bifunctional $KD1_{L17R}$-K_T is effective in reducing blood loss in mouse tail-amputation and liver-laceration hemorrhage models [29]. Although these mouse models have limitations as compared to the extremity trauma and internal organ

hemorrhage in humans, these models are suitable for initial testing the potency of $KD1_{L17R}$-K_T. However, appropriately expressed $KD1_{L17R}$-K_T without the His-tag and with intact C-terminal Lys is essential such that proteolysis is eliminated after purification. We are currently exploring several possibilities for expressing such $KD1_{L17R}$-K_T molecules with one or two additional mutations to perform dose dependent studies in order to test their efficacies.

Supplementary Material

Refer to Web version on PubMed Central for supplementary material.

Acknowledgments

We thank Dr. Philip Liu of Orthopaedic Surgery and Dr. Joni Ricks-Oddie of UCLA IDRE for Statistical Consulting Services. This work was supported, in part, by National Heart, Lung and Blood Institute grant 5R21HL122878.

References

1. Grant, MA., Aird, WC. Molecular evolution of the vertebrate blood coagulation system Thrombosisand Hemostasis: Basic principles & clinical practice. 6. Marder, VJ.Aird, WC.Bennett, JS.Schulman, S., White, GC., II, editors. Lippincott: Williams & Wilkins; 2012. p. 11-25.
2. Urano S, Metzger AR, Castellino FJ. Plasmin-mediated fibrinolysis by variant recombinant tissue plasminogen activators. Proc Natl Acad Sci USA. 1989; 86:2568–71. [PubMed: 2523073]
3. Plow EF, Herren T, Redlitz A, Miles LA, Hoover-Plow JL. The cell biology of the plasminogen system. FASEB J. 1995; 9:939–45. [PubMed: 7615163]
4. Kashuk JL, Moore EE, Sawyer M, Wohlauer M, Pezold M, Barnett C, Biffl WL, Burlew CC, Johnson JL, Sauaia A. Primary fibrinolysis is integral in the pathogenesis of the acute coagulopathy of trauma. Ann Surg. 2010; 252:434–42. [PubMed: 20739843]
5. Raza I, Davenport R, Rourke C, Platton S, Manson J, Spoors C, Khan S, De'Ath HD, Allard S, Hart DP, Pasi KJ, Hunt BJ, Stanworth S, MacCallum PK, Brohi K. The incidence and magnitude of fibrinolytic activation in trauma patients. J Thromb Haemost. 2013; 11:307–14. [PubMed: 23176206]
6. Cardenas JC, Wade CE, Holcomb JB. Mechanisms of trauma-induced coagulopathy. Curr Opin Hematol. 2014; 21:404–9. [PubMed: 25010798]
7. Boucher BA, Hannon TJ. Blood management: a primer for clinicians. Pharmacotherapy. 2007; 27:1394–411. [PubMed: 17896895]
8. Hendrickson JE, Hillyer CD. Noninfectious serious hazards of transfusion. Anesth Analg. 2009; 108:759–69. [PubMed: 19224780]
9. Ker K, Roberts I, Shakur H, Coats TJ. Antifibrinolytic drugs for acute traumatic injury. Cochrane Database Syst Rev. 2015:CD004896. [PubMed: 25956410]
10. Koster A, Faraoni D, Levy JH. Antifibrinolytic Therapy for Cardiac Surgery: An Update. Anesthesiology. 2015; 123:214–21. [PubMed: 25950230]
11. Hartmann M, Sucker C, Boehm O, Koch A, Loer S, Zacharowski K. Effects of cardiac surgery on hemostasis. Transfusion Med Rev. 2006; 20:230–41.
12. Fergusson DA, Hebert PC, Mazer CD, Fremes S, MacAdams C, Murkin JM, Teoh K, Duke PC, Arellano R, Blajchman MA, Bussieres JS, Cote D, Karski J, Martineau R, Robblee JA, Rodger M, Wells G, Clinch J, Pretorius R. BART Investigators. A comparison of aprotinin and lysine analogues in high-risk cardiac surgery. N Engl J Med. 2008; 358:2319–31. [PubMed: 18480196]
13. Sharma V, Katznelson R, Jerath A, Garrido-Olivares L, Carroll J, Rao V, Wasowicz M, Djaiani G. The association between tranexamic acid and convulsive seizures after cardiac surgery: a multivariate analysis in 11529 patients. Anaesthesia. 2014; 69:124–30. [PubMed: 24588023]

14. Lecker I, Wang DS, Whissell PD, Avramescu S, Mazer CD, Orser BA. Tranexamic acid-associated seizures: Causes and treatment. Ann Neurol. 2016; 79:18–26. [PubMed: 26580862]
15. Martin K, Wiesner G, Breuer T, Lange R, Tassani P. The risks of aprotinin and tranexamic acid in cardiac surgery: a one-year follow-up of 1188 consecutive patients. Anesth Analg. 2008; 107:1783–90. [PubMed: 19020118]
16. Breuer T, Martin K, Wilhelm M, Wiesner G, Schreiber C, Hess J, Lange R, Tassani P. The blood sparing effect and the safety of aprotinin compared to tranexamic acid in paediatric cardiac surgery. Eur J Cardiothorac Surg. 2009; 35:167–71. [PubMed: 19027313]
17. Sander M, Spies CD, Martiny V, Rosenthal C, Wernecke KD, von Heymann C. Mortality associated with administration of high-dose tranexamic acid and aprotinin in primary open-heart procedures: a retrospective analysis. Crit Care. 2010; 14:R148. [PubMed: 20682059]
18. Martin K, Knorr J, Breuer T, Gertler R, Macguill M, Lange R, Tassani P, Wiesner G. Seizures after open heart surgery: comparison of ε-aminocaproic acid and tranexamic acid. J Cardiothorac Vasc Anesth. 2011; 25:20–5. [PubMed: 21272777]
19. Montes FR, Pardo DF, Carreño M, Arciniegas C, Dennis RJ, Umaña JP. Risk factors associated with postoperative seizures in patients undergoing cardiac surgery who received tranexamic acid: A case-control study. Ann Card Anaesth. 2012; 15:6–12. [PubMed: 22234015]
20. Makhija N, Sarupria A, Kumar Choudhary S, Das S, Lakshmy R, Kiran U. Comparison of epsilon aminocaproic acid and tranexamic Acid in thoracic aortic surgery: clinical efficacy and safety. J Cardiothorac Vasc Anesth. 2013; 27:1201–7. [PubMed: 24050855]
21. Shaw AD, Stafford-Smith M, White WD, Phillips-Bute B, Swaminathan M, Milano C, Welsby IJ, Aronson S, Mathew JP, Peterson ED, Newman MF. The effect of aprotinin on outcome after coronary-artery bypass grafting. N Engl J Med. 2008; 358:784–93. [PubMed: 18287601]
22. Rabinovici R, Heyman A, Kluger Y, Shinar E. Convulsions induced by aminocaproic acid infusion. DICP. 1989; 23:780–1. [PubMed: 2815855]
23. Lenfors S, Gustafsson D. New model for in vivo studies of pharmacological interventions with endogenous fibrinolysis: effects of thrombin inhibitors. Semin Thromb Hemost. 1996; 22:335–42. [PubMed: 8944418]
24. Mao SS, Holahan MA, Bailey C, Wu G, Colussi D, Carroll SS, Cook JJ. Demonstration of enhanced endogenous fibrinolysis in thrombin activatable fibrinolysis inhibitor-deficient mice. Blood Coagul Fibrinolysis. 2005; 16:407–15. [PubMed: 16093731]
25. Paul J, Strickland S, Melchor JP. Fibrin deposition accelerates neurovascular damage and neuroinflammation in mouse models of Alzheimer's disease. J Exp Med. 2007; 204:1999–2008. [PubMed: 17664291]
26. Bruno NE, Yano Y, Takei Y, Gabazza EC, Qin L, Nagashima M, Morser J, D'Alessandro-Gabazza CN, Taguchi O, Sumida Y. Protective role of thrombin activatable fibrinolysis inhibitor in obstructive nephropathy-associated tubulointerstitial fibrosis. J Thromb Haemost. 2008; 6:139–46. [PubMed: 17988229]
27. Kłak M, Anakkala N, Wang W, Lange S, Jonsson IM, Tarkowski A, Jin T. Tranexamic acid, an inhibitor of plasminogen activation, aggravates staphylococcal septic arthritis and sepsis. Scand J Infect Dis. 2010; 42:351–8. [PubMed: 20100112]
28. Lecker I, Wang DS, Romaschin AD, Peterson M, Mazer CD, Orser BA. Tranexamic acid concentrations associated with human seizures inhibit glycine receptors. J Clin Invest. 2012; 122:4654–66. [PubMed: 23187124]
29. Kumar Y, Vadivel K, Schmidt AE, Ogueli GI, Ponnuraj SM, Rannulu N, Loo JA, Bajaj MS, Bajaj SP. Decoy plasminogen receptor containing a selective Kunitz-inhibitory domain. Biochemistry. 2014; 53:505–17. [PubMed: 24383758]
30. Schlag MG, Hopf R, Redl H. Convulsive seizures following subdural application of fibrin sealant containing tranexamic acid in a rat model. Neurosurgery. 2000; 47:1463–7. [PubMed: 11126922]
31. Furtmüller R, Schlag MG, Berger M, Hopf R, Huck S, Sieghart W, Redl H. Tranexamic acid, a widely used antifibrinolytic agent, causes convulsions by a gamma-aminobutyric $acid_A$ receptor antagonistic effect. J Pharmacol Exp Ther. 2002; 301:168–73. [PubMed: 11907171]

32. Yamaura A, Nakamura T, Makino H, Hagihara Y. Cerebral complication of antifibrinolytic therapy in the treatment of ruptured intracranial aneurysm. Animal experiment and a review of literature. Eur Neurol. 1980; 19:77–84. [PubMed: 6893025]
33. Pellegrini A, Giaretta D, Chemello R, Zanotto L, Testa G. Feline generalized epilepsy induced by tranexamic acid (AMCA). Epilepsia. 1982; 23:35–45. [PubMed: 7056249]
34. Bajaj MS, Ogueli GI, Kumar Y, Vadivel K, Lawson G, Shanker S, Schmidt AE, Bajaj SP. Engineering Kunitz domain 1 (KD1) of human tissue factor pathway inhibitor-2 to selectively inhibit fibrinolysis: properties of KD1-L17R variant. J Biol Chem. 2011; 286:4329–40. [PubMed: 21115497]
35. Kempaiah P, Danielson LA, Barry M, Kisiel W. Comparative effects of aprotinin and human recombinant R24K KD1 on temporal renal function in Long-Evans rats. J Pharmacol Exp Ther. 2009; 331:940–5. [PubMed: 19776384]
36. Markus G, DePasquale JL, Wissler FC. Quantitative determination of the binding of epsilon-aminocaproic acid to native plasminogen. J Biol Chem. 1978; 253:727–32. [PubMed: 621200]
37. Mathews II, Vanderhoff-Hanaver P, Castellino FJ, Tulinsky A. Crystal structures of the recombinant kringle 1 domain of human plasminogen in complexes with the ligands epsilon-aminocaproic acid and trans-4-(aminomethyl)cyclohexane-1-carboxylic Acid. Biochemistry. 1996; 35:2567–76. [PubMed: 8611560]
38. Markland W, Ley AC, Lee SW, Ladner RC. Iterative optimization of high-affinity proteases inhibitors using phage display. 1. Plasmin. Biochemistry. 1996; 35:8045–57. [PubMed: 8672509]
39. Dietrich W, Nicklisch S, Koster A, Spannagl M, Giersiefen H, van de Locht A. CU-2010--a novel small molecule protease inhibitor with antifibrinolytic and anticoagulant properties. Anesthesiology. 2009; 110:123–30. [PubMed: 19104179]
40. Flight SM, Johnson LA, Du QS, Warner RL, Trabi M, Gaffney PJ, Lavin MF, de Jersey J, Masci PP. Textilinin-1, an alternative anti-bleeding agent to aprotinin: Importance of plasmin inhibition in controlling blood loss. Br J Haematol. 2009; 145:207–11. [PubMed: 19236611]
41. Swedberg JE, Harris JM. Plasmin substrate binding site cooperativity guides the design of potent peptide aldehyde inhibitors. Biochemistry. 2011; 50:8454–62. [PubMed: 21877690]
42. Bokesch PM, Szabo G, Wojdyga R, Grocott HP, Smith PK, Mazer CD, Vetticaden S, Wheeler A, Levy JH. A phase 2 prospective, randomized, double-blind trial comparing the effects of tranexamic acid with ecallantide on blood loss from high-risk cardiac surgery with cardiopulmonary bypass (CONSERV-2 Trial). J Thorac Cardiovasc Surg. 2012; 143:1022–9. [PubMed: 21724197]
43. Saupe SM, Leubner S, Betz M, Klebe G, Steinmetzer T. Development of new cyclic plasmin inhibitors with excellent potency and selectivity. J Med Chem. 2013; 56:820–31. [PubMed: 23294255]
44. Englberger L, Dietrich W, Eberle B, Erdoes G, Keller D, Carrel T. A novel blood-sparing agent in cardiac surgery? First in-patient experience with the synthetic serine protease inhibitor MDCO-2010: A phase II, randomized, double-blind, placebo-controlled study in patients undergoing coronary artery bypass grafting with cardiopulmonary bypass. Anesth Analg. 2014; 119:16–25. [PubMed: 24722261]
45. Cheng L, Pettersen D, Ohlsson B, Schell P, Karle M, Evertsson E, Pahlen S, Jonforsen M, Plowright AT, Bostrom J, Fex T, Thelin A, Hilgendorf C, Xue Y, Wahlund G, Lindberg W, Larsson LO, Gustafsson D. Discovery of the Fibrinolysis Inhibitor AZD6564, Acting via Interference of a Protein-Protein Interaction. ACS Med Chem Lett. 2014; 5:538–43. [PubMed: 24900876]
46. Al-Horani RA, Desai UR. Recent advances on plasmin inhibitors for the treatment of fibrinolysis-related disorders. Med Res Rev. 2014; 34:1168–216. [PubMed: 24659483]
47. de Veer SJ, Wang CK, Harris JM, Craik DJ, Swedberg JE. Improving the Selectivity of Engineered Protease Inhibitors: Optimizing the P2 Prime Residue Using a Versatile Cyclic Peptide Library. J Med Chem. 2015; 58:8257–68. [PubMed: 26393374]
48. Masci PP, Whitaker AN, Sparrow LG, de Jersey J, Winzor DJ, Watters DJ, Lavin MF, Gaffney PJ. Textilinins from Pseudonaja textilis textilis. Characterization of two plasmin inhibitors that reduce bleeding in an animal model. Blood Coagul Fibrinolysis. 2000; 11:385–93. [PubMed: 10847427]

49. Jankun J, Keck R, Selman SH, Skrzypczak-Jankun E. Systemic or topical application of plasminogen activator inhibitor with extended half-life (VLHL PAI-1) reduces bleeding time and total blood loss. Int J Mol Med. 2010; 26:501–4. [PubMed: 20818488]
50. Laemmli UK. Cleavage of structural proteins during assembly of head of bacteriophage-t4. Nature. 1970; 227:680–5. [PubMed: 5432063]
51. Chand HS, Schmidt AE, Bajaj SP, Kisiel W. Structure-function analysis of the reactive site in the first Kunitz-type domain of human tissue factor pathway inhibitor-2. J Biol Chem. 2004; 279:17500–7. [PubMed: 14970225]
52. Schmidt AE, Chand HS, Cascio D, Kisiel W, Bajaj SP. Crystal structure of Kunitz domain 1 (KD1) of tissue factor pathway inhibitor-2 in complex with trypsin. Implications for KD1 specificity of inhibition. J Biol Chem. 2005; 280:27832–8. [PubMed: 15932872]
53. Beith JG. In vivo significance of kinetic constants of protein proteinase inhibitors. Biochem Med. 1984; 32:387–97. [PubMed: 6517881]
54. Morrison JF, Walsh CT. The behavior and significance of slow-binding enzyme inhibitors. Adv Enzymol Relat Areas Mol Biol. 1988; 61:201–301. [PubMed: 3281418]
55. Bojar, RM. Manual of perioperative care in adult cardiac surgery. 4. Blackwell Publishing, Hoboken; New Jersey: 2005. Cardiac Anesthesia; p. 129-178.
56. Nilsson IM. Clinical pharmacology of aminocaproic and tranexamic acids. J Clin Pathol Suppl (R Coll Pathol). 1980; 14:41–7. [PubMed: 7000846]
57. Broze GJ Jr, Yin ZF, Lasky N. A tail vein bleeding time model and delayed bleeding in hemophiliac mice. Thromb Haemost. 2001; 85:747–8. [PubMed: 11341518]
58. [Accessed 8 September 2016] Australian public assessment report for tranexamic acid. Cyklokapran. https://www.tga.gov.au/sites/default/files/auspar-cyklokapron.pdf
59. [Accessed 25 July 2016] Trasylol. http://www.accessdata.fda.gov/drugsatfda_docs/label/2006/020304s022lbl.pdf
60. Farkas H, Varga L. Ecallantide is a novel treatment for attacks of hereditary angioedema due to C1 inhibitor deficiency. Clin Cosmet Investig Dermatol. 2011; 4:61–8.
61. Markwardt, F. Naturally occurring inhibitors of fibrinolysis. In: Markwardt, F., editor. Fibrinolytics and Anti-fibrinolytics. Springer-Verlag; 1978. p. 487-509.
62. Eswar N, Webb B, Marti-Renom MA, Madhusudhan MS, Eramian D, Shen MY, Pieper U, Sali A. Comparative Protein Structure Modeling With MODELLER. Current Protocols in Bioinformatics, John Wiley & Sons. 2006; (Supplement 15):5.6.1–30.
63. Berman HM, Westbrook J, Feng Z, Gilliland G, Bhat TN, Weissig H, Shindyalov IN, Bourne PE. The Protein Data Bank. Nucleic Acids Res. 2000; 28:235–42. www.rcsb.org. [PubMed: 10592235]
64. Brooks BR, Brooks CL 3rd, Mackerell AD Jr, Nilsson L, Petrella RJ, Roux B, Won Y, Archontis G, Bartels C, Boresch S, Caflisch A, Caves L, Cui Q, Dinner AR, Feig M, Fischer S, Gao J, Hodoscek M, Im W, Kuczera K. CHARMM: the biomolecular simulation program. J Comput Chem. 2009; 30:1545–614. [PubMed: 19444816]
65. Baker NA, Sept D, Joseph S, Holst MJ, McCammon JA. Electrostatics of nanosystems: application to microtubules and the ribosome. Proc Natl Acad Sci USA. 2001; 98:10037–41. [PubMed: 11517324]
66. The PyMOL Molecular Graphics System, Version 1.8 Schr00F6dinger, LLC.
67. Fritz H, Wunderer G. Biochemistry and applications of aprotinin, the kallikrein inhibitor from bovine organs. Arzneimittelforschung/Drug Res. 1983; 33:479–94. [PubMed: 6191764]
68. Petersen TE, Martzen MR, Ichinose A, Davie EW. Characterization of the gene for human plasminogen, a key proenzyme in the fibrinolytic system. J Biol Chem. 1990; 265:6104–11. [PubMed: 2318848]
69. Degen SJ, Bell SM, Schaefer LA, Elliott RW. Characterization of the cDNA coding for mouse plasminogen and localization of the gene to mouse chromosome 17. Genomics. 1990; 8:49–61. [PubMed: 2081600]
70. Marquart M, Walter J, Deisenhofer J, Bode W, Huber R. The geometry of the reactive site and of the peptide groups in trypsin, trypsinogen and its complexes with inhibitors. Acta Cryst. 1983; B39:480–90.

71. Fujikawa K, Chung DW, Hendrickson LE, Davie EW. Amino acid sequence of human factor XI, a blood coagulation factor with four tandem repeats that are highly homologous with plasma prekallikrein. Biochemistry. 1986; 25:2417–24. [PubMed: 3636155]

72. Gailani D, Sun MF, Sun Y. A comparison of murine and human factor XI. Blood. 1997; 90:1055–64. [PubMed: 9242536]

73. Chung DW, Fujikawa K, McMullen BA, Davie EW. Human plasma prekallikrein, a zymogen to a serine protease that contains four tandem repeats. Biochemistry. 1986; 25:2410–7. [PubMed: 3521732]

74. Seidah NG, Sawyer N, Hamelin J, Mion P, Beaubien G, Brachpapa L, Rochemont J, Mbikay M, Chrétien M. Mouse plasma kallikrein: cDNA structure, enzyme characterization, and comparison of protein and mRNA levels among species. DNA Cell Biol. 1990; 9:737–48. [PubMed: 2264928]

75. Lay AJ, Liang Z, Rosen ED, Castellino FJ. Mice with a severe deficiency in protein C display prothrombotic and proinflammatory phenotypes and compromised maternal reproductive capabilities. J Clin Invest. 2005; 115:1552–61. [PubMed: 15902301]

Essentials

Current antifibrinolytics—Aminocaproic acid and tranexamic acid can cause seizures or renal injury

$KD1_{L17R}$-K_T, aprotinin and tranexamic acid were tested in a modified mouse tail-amputation model

S2′-subsite variations between human and mouse FXIa result in vastly different inhibition profiles

$KD1_{L17R}$-K_T reduces blood loss and D-dimer levels in mouse with unobserved seizures or renal injury

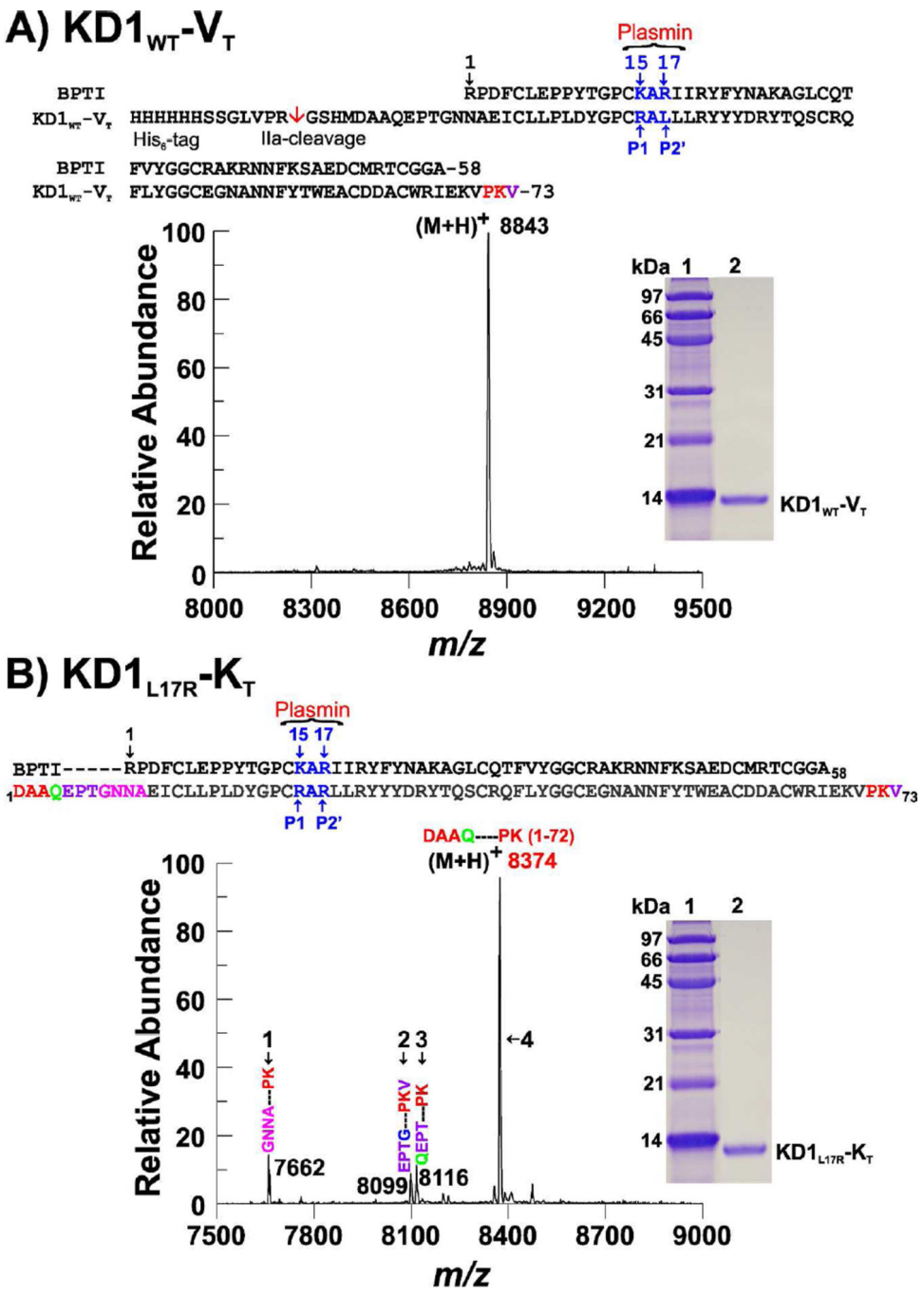

Fig. 1. SDS-PAGE, MALDI-TOF-ESI mass spectrometry and amino acid sequences of $KD1_{WT}$-V_T and $KD1_{L17R}$-K_T

Mass spectrometry data were obtained using an Applied Biosystems Voyager DE-STR. (A) *$KD1_{WT}$-V_T*. The mass was 8843 Da and the N-terminal sequence was GSHMDAA at ~80 pmol level. Combined mass spectrometry and sequence data reveal EKVPKV sequence at the C-terminus of $KD1_{WT}$-V_T. For comparison, amino acid sequence alignment of $KD1_{WT}$-V_T with BPTI is presented to indicate that the residue Asn10 in $KD1_{WT}$-V_T represents residue Arg1 in BPTI. Thus, $KD1_{WT}$-V_T has nine extra residues at the N-terminus excluding GSHM. The P1 residue Arg (15 in BPTI numbering, residue 24 in $KD1_{WT}$-V_T) and P2′

residue Arg (17 in BPTI and 26 in $KD1_{WT}$-V_T) are indicated. Inset, SDS-PAGE (15% acrylamide). Lane 1, reduced EZ-Run protein markers (Fisher Bioreagents); lane 2, reduced $KD1_{WT}$-V_T (5 μg). (B) *$KD1_{L17R}$-K_T*. Mass spectrometry revealed three minor (peaks 1–3, ~8% each) and one major molecular species (peak 4, ~75%). The N-terminal sequence was DAAQEPT at the ~90 pmol level and the other N-terminal sequences (Cycle 1, ~8 pmol; cycle 2, ~6 pmol and cycle 3, ~5 pmol) were QEP, EPT and GNN. Combined mass spectrometry and sequence data revealed that the three molecular species (peaks 1, 3 and 4) each has C-terminal Lys72 and constitutes ~92% of the total mass; only peak 2 (~8%) has C-terminal Val73. The difference in molecular mass results from proteolysis by IIa or a contaminating protease. For comparison, the sequence alignment of $KD1_{L17R}$-K_T with BPTI is given. Inset, SDS-PAGE (15% acrylamide). Lane 1, reduced EZ-Run protein markers; lane 2, reduced $KD1_{L17R}$-K_T (5 μg).

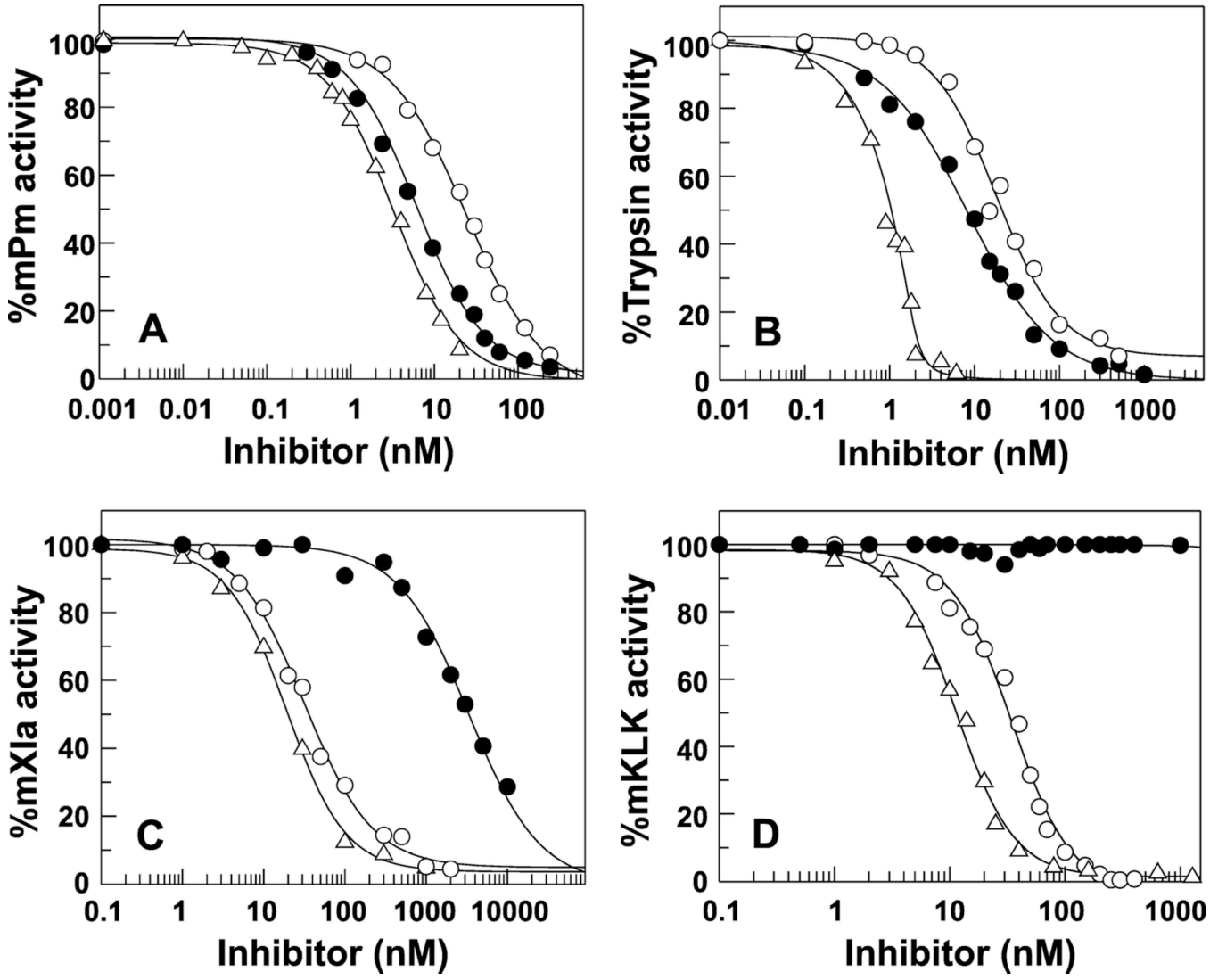

Fig. 2. Determination of equilibrium inhibition constants (K_i) of $KD1_{WT}$-V_T, $KD1_{L17R}$-K_T, and aprotinin with mPm, mXIa, mKLK and bovine trypsin

(A) *P*ercent activity of 3 nM mPm remaining in the presence of various concentrations of $KD1_{L17R}$-K_T (●), $KD1_{WT}$-V_T (o) and aprotinin (△). (B) Percent activity of 2 nM bovine trypsin remaining in the presence of various concentrations of $KD1_{L17R}$-K_T (●), $KD1_{WT}$-V_T (o), and aprotinin (△). (C) Percent activity of 1 nM mXIa remaining in the presence of various concentrations of $KD1_{L17R}$-K_T (●), $KD1_{WT}$-V_T (o), and aprotinin (△). (D) Percent activity of 1 nM mKLK remaining in the presence of various concentrations of $KD1_{L17R}$-K_T (●), $KD1_{WT}$-V_T (o), and aprotinin (△).

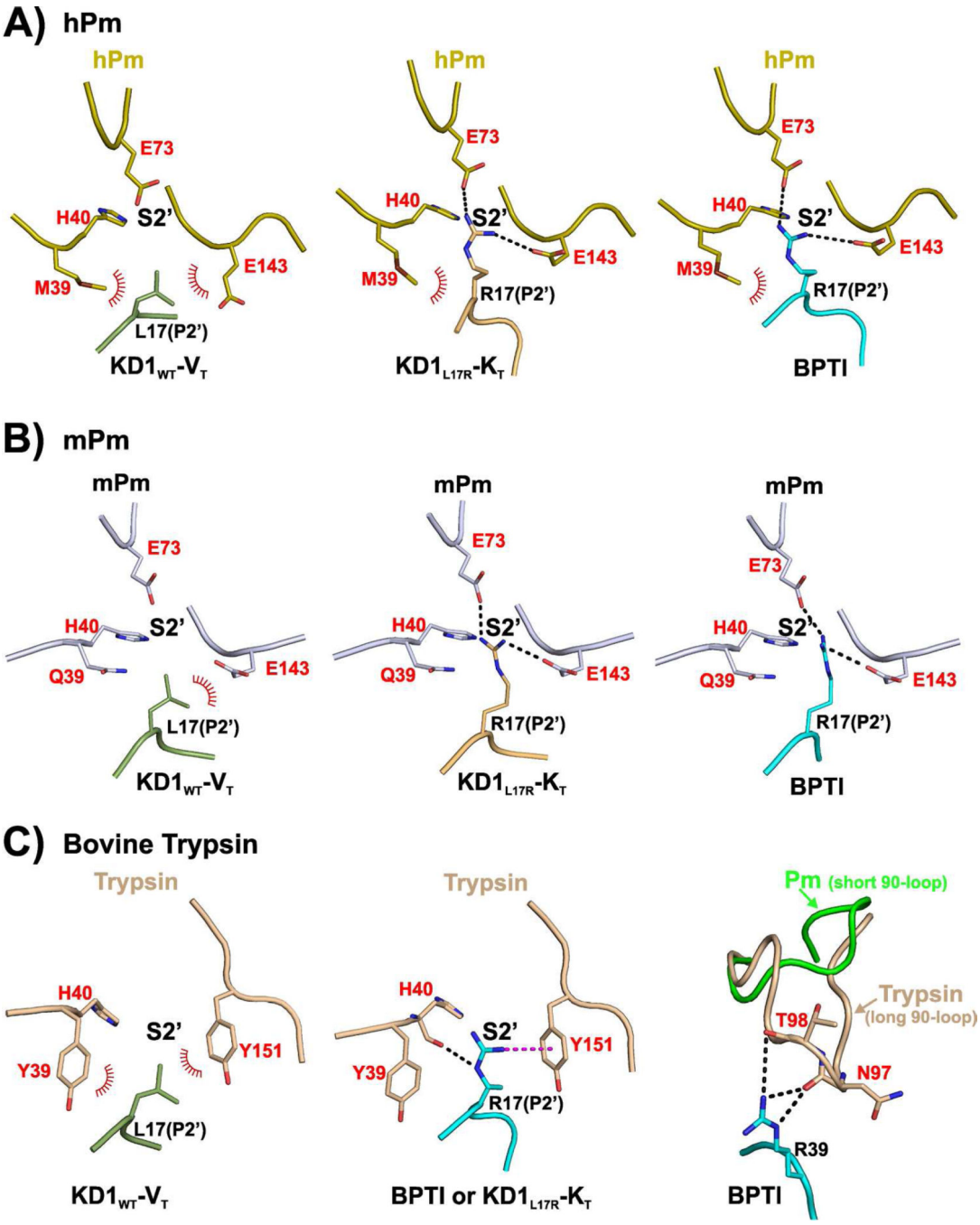

Fig. 3. Interactions between the protease domains each of hPm, mPm and bovine trypsin with $KD1_{WT}$-V_T, $KD1_{L17R}$-K_T and BPTI

(A) Interaction between the P2′ residue of $KD1_{WT}$-V_T, $KD1_{L17R}$-K_T or BPTI with S2′-pocket of hPm. Left, hydrophobic interactions between Leu17 of $KD1_{WT}$-V_T with Met39 and Glu143 hydrocarbon side chain of hPm. Middle, salt-bridge interactions of Arg17 of $KD1_{L17R}$-K_T with Glu73 and Glu143 as well as hydrophobic contacts with Met39 of hPm. Right, similar to $KD1_{L17R}$-K_T, interactions of Arg17 of BPTI with Glu73/Glu143 and Met39 of hPm. (B) Interaction between P2′ residue of $KD1_{WT}$-V_T, $KD1_{L17R}$-K_T or BPTI with S2′-pocket of mPm. Left, hydrophobic contact between Leu17 of $KD1_{WT}$-V_T and

Glu143 side chain of mPm. Middle, interactions between Arg17 of $KD1_{L17R}$-K_T involving salt-bridge with Glu73 and Glu143 of mPm. Right, similar to $KD1_{L17R}$-K_T, interactions of Arg17 of BPTI with Glu73/Glu143 of mPm. (C) Interaction between the P2′ residue of $KD1_{WT}$-V_T, $KD1_{L17R}$-K_T or BPTI with S2′-pocket of trypsin and additional interactions of trypsin with BPTI. Left, hydrophobic interactions between Leu17 of $KD1_{WT}$-V_T with Tyr39 and Tyr151 of trypsin. Middle, interactions of Arg17 of $KD1_{L17R}$-K_T or BPTI involving π-interactions with Tyr151 and hydrogen bond with His40 main chain of trypsin. Right, additional hydrogen bond interactions between Arg39 of BPTI with Thr98 and Asn97 of trypsin. hPm or mPm 90-loop (green) is short and has no interactions with BPTI. $KD1_{WT}$-VT is shown in dark green, $KD1_{L17R}$-K_T in sand, BPTI in cyan, hPm in dark yellow, mPm in light blue and trypsin in wheat. The hydrogen bonds are shown in black dashed lines, π-interaction in magenta dashed line and the hydrophobic interactions by arcs with spokes radiating toward the contact atoms.

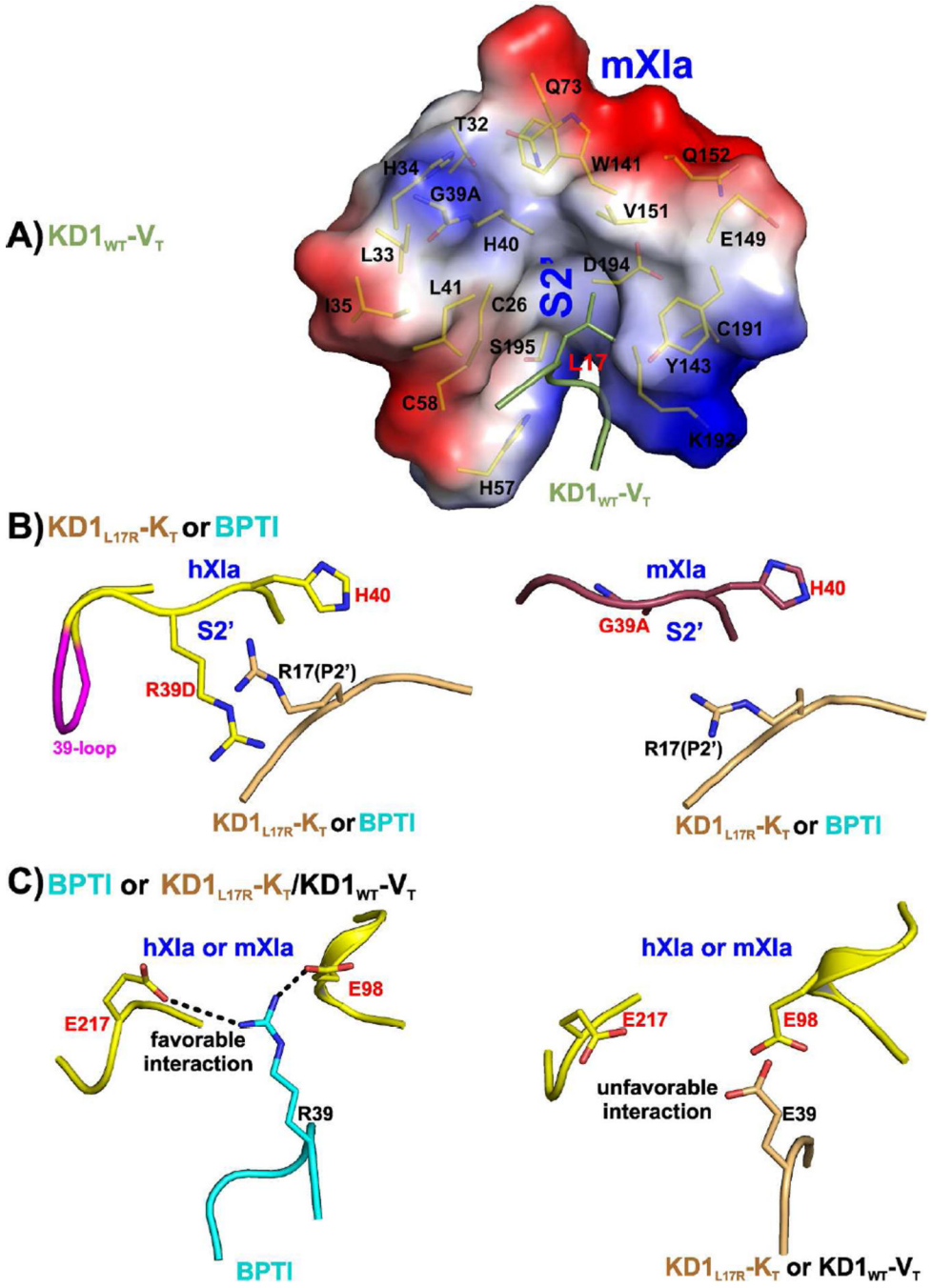

Fig. 4. Modeled interactions between the protease domains each of mXIa and hXIa with $KD1_{WT}$-V_T, $KD1_{L17R}$-K_T and BPTI

(A) Interaction between P2′ Leu17 of $KD1_{WT}$-V_T with S2′-pocket of mXIa. Similar to hXIa [34], Leu17 of $KD1_{WT}$-V_T is situated in a vastly hydrophobic S2′-pocket environment of mXIa. Pymol generated map of the electrostatic potential at the solvent-accessible surface of the mXIa catalytic domain near residue Leu17 of $KD1_{WT}$-V_T is shown. The mXIa residues within 6 A radius of Leu17 of $KD1_{WT}$-V_T were selected for display. Blue represents positive, red represents negative and white represents hydrophobic surface potential. (B) P2′ Arg17 of BPTI or $KD1_{L17R}$-K_T and S2′-pockets of hXIa and mXIa. Left,

the longer 39-loop and the presence of Arg39D in hXIa disfavor the interaction with Arg17 of BPTI or $KD1_{L17R}$-K_T. Right, the short 39-loop and the absence of a basic residue in mXIa relieves the repulsive interaction with Arg17 of BPTI or $KD1_{L17R}$-K_T. The capital letter followed by the residue number, e.g., R39D or G39A indicates insertion. (C) Additional interactions of hXIa (or mXIa) with BPTI and their absence in $KD1_{WT}$-V_T or $KD1_{L17R}$-K_T. Left, Arg39 of BPTI makes salt-bridge with Glu98 and Glu217 of hXIa or mXIa. Right, the presence of Glu39 in $KD1_{WT}$-V_T or $KD1_{L17R}K_T$ disfavor these interactions.

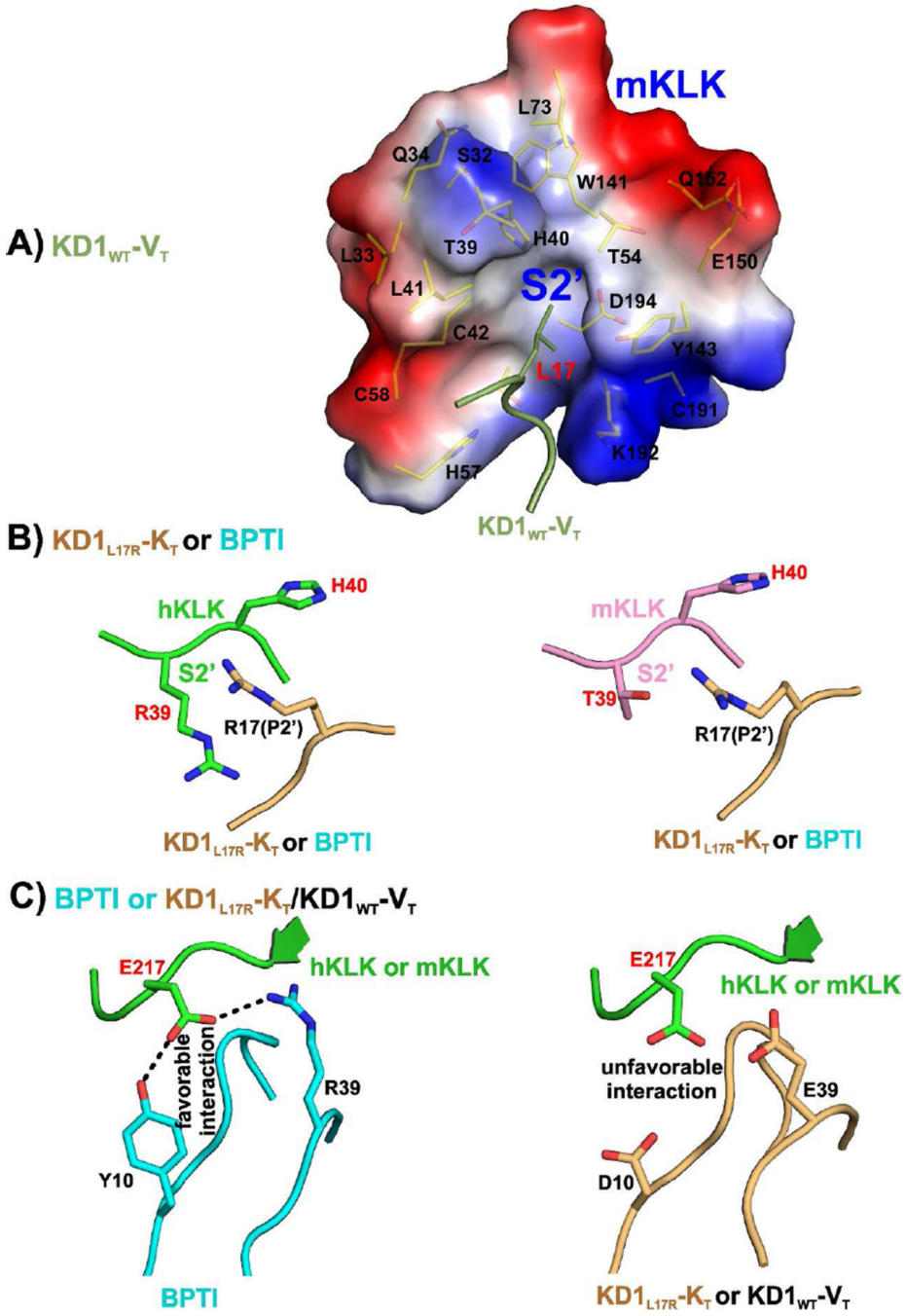

Fig. 5. Modeled interactions between the protease domains each of mKLK and hKLK with $KD1_{WT}$-V_T, $KD1_{L17R}$-K_T and BPTI

(A) Interaction between P2′ Leu17 of $KD1_{WT}$-V_T with S2′-pocket of mKLK. Similar to hKLK [34], Leu17 of $KD1_{WT}$-V_T is situated in a vastly hydrophobic S2′-pocket environment of mKLK. Pymol generated map of the electrostatic potential at the solvent-accessible surface of the mKLK catalytic domain near residue Leu17 of $KD1_{WT}$-V_T is shown. The mKLK residues within 6 A radius of Leu17 of $KD1_{WT}$-V_T were selected for display. Blue represents positive, red represents negative and white represents hydrophobic surface potential. (B) P2′ Arg17 of BPTI or $KD1_{L17R}$-K_T and S2′-pockets of hKLK and

mKLK. Left, Arg39 in hKLK unfavorable for interaction with Arg17 of BPTI or $KD1_{L17R}$-K_T. Right, Short side chain of Thr39 in mKLK can accommodate Arg17 of BPTI or $KD1_{L17R}$-K_T. (C) Additional interactions of hKLK (or mKLK) with BPTI and their absence in $KD1_{WT}$-V_T or $KD1_{L17R}$-K_T. Left, Tyr10 and Arg39 of BPTI make hydrogen bond and a salt-bridge with Glu217 of hKLK or mKLK. Right, the presence of Asp10 and Glu39 in $KD1_{WT}$-V_T or $KD1_{L17R}$-K_T disfavor these interactions.

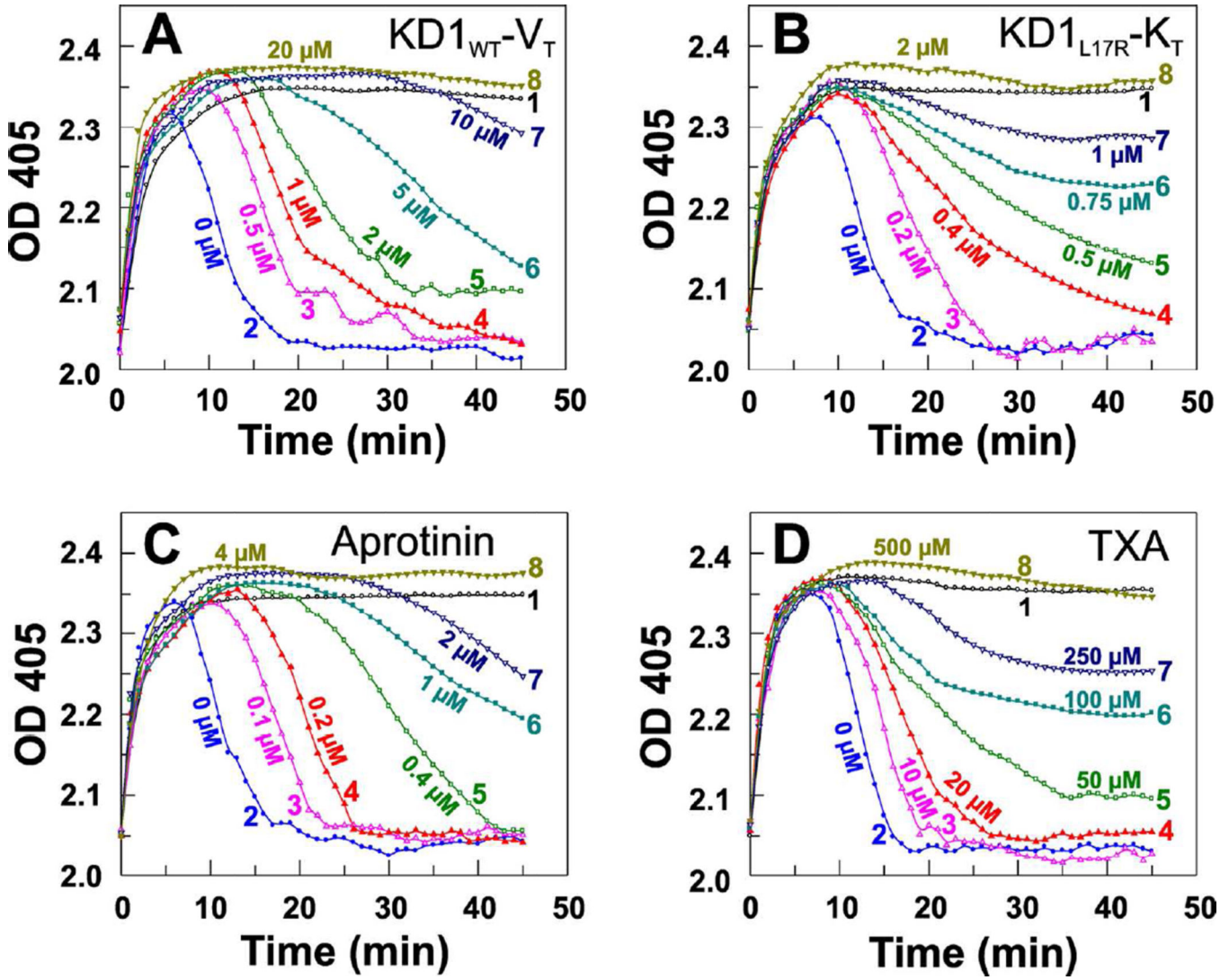

Fig. 6. Effect of $KD1_{WT}$-V_T, $KD1_{L17R}$-K_T, aprotinin or TXA on fibrinolysis in mouse plasma

IIa was added to mouse plasma to initiate clot formation, which is associated with an increase in OD_{405} (curve 1 in A–D, o). Simultaneously added tPA converted plasminogen to Pm, which dissolved the fibrin clot completely within ~18 min, as indicated by an initial increase followed by a decrease in OD_{405} (curve 2 in A–D, ●). Addition of $KD1_{WT}$-V_T, $KD1_{L17R}$-K_T, aprotinin or TXA inhibited fibrinolysis in a dose dependent manner. (A) Effect of $KD1_{WT}$-V_T; 0.5 μM (curve 3△), 1 μM (curve 4▲), 2 μM (curve 5□), 5 μM, (curve 6■), 10 μM (curve 7▽), and 20 μM (curve 8▼). (B) Effect of $KD1_{L17R}$-K_T; 0.2 μM (curve 3△), 0.4 μM (curve 4▲), 0.5 μM (curve 5□), 0.75 μM, (curve 6■), 1 μM (curve 7▽), and 2 μM (curve 8▼). (C) Effect of aprotinin; 0.1 μM (curve 3△), 0.2 μM (curve 4▲), 0.4 μM (curve 5□), 1 μM, (curve 6■), 2 μM (curve 7▽), and 4 μM (curve 8▼). (D) Effect of TXA; 10 μM (curve 3△), 20 μM (curve 4▲), 50 μM (curve 5□), 100 μM, (curve 6■), 250 μM (curve 7▽), and 500 μM (curve 8▼).

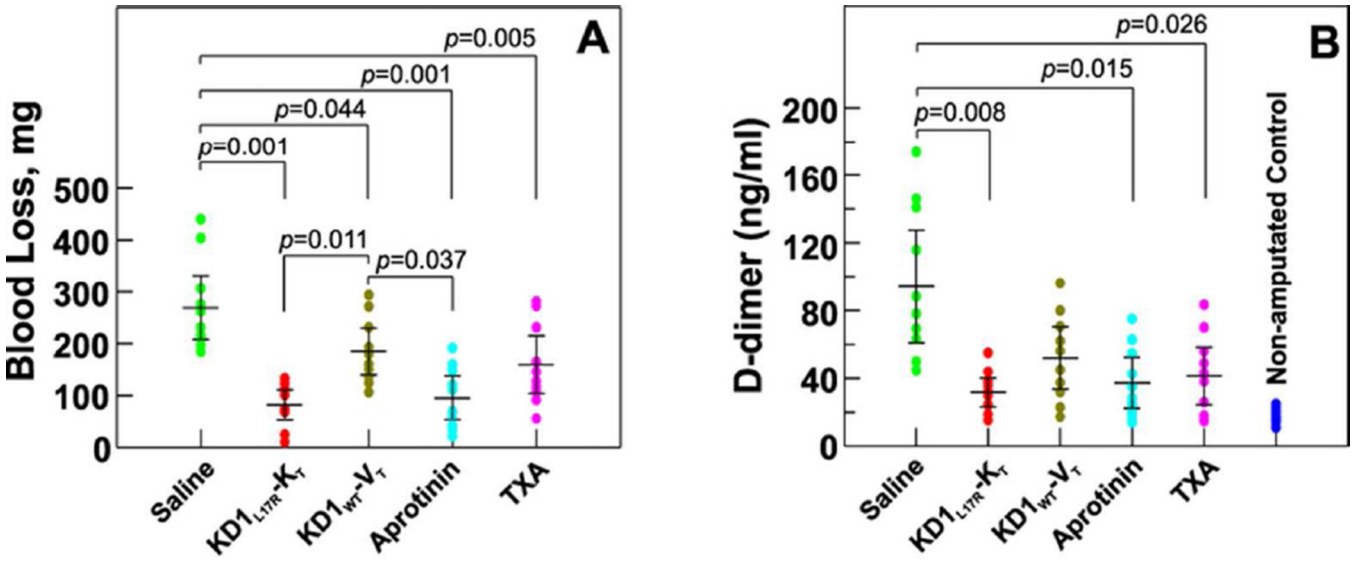

Fig. 7. Effect of $KD1_{WT}$-V_T, $KD1_{L17R}$-K_T, aprotinin, and TXA in tail-amputation haemorrhage model

Animals were treated with saline, $KD1_{WT}$-V_T, $KD1_{L17R}$-K_T, aprotinin or TXA by intravenous bolus injection. The antifibrinolytic agents and saline were free of lipopolysaccharide, as tested using the Limulus amebocyte lysates kit (Bio Whittaker Inc., Walkersville, MD). After allowing two minutes for circulation of the drug, the tail was amputated at 4 cm from the tip using a sharp, sterile, #11 scalpel blade. Blood was allowed to flow freely and drip into preweighed eppendorf tubes. Total blood loss was the difference in the weight of eppendorf tube before and after blood collection. At the end of the experiment, citrated blood samples were obtained from lateral saphenous vein for D-dimer assay by venipuncture. Blood was processed immediately to obtain plasma. The plasma D-dimer concentration was measured using the Asserachrom D-Di kit from Diagnostica Stago. Scatter plot showing blood loss (A) and D-dimer levels (B) in different groups. Black bars represent the mean and the 95% CI (confidence interval). Tukey and Games-Howell post-hoc tests were used to obtain *p*-values between the different groups for blood loss and the D-dimer levels, respectively. The *p*-values that are significant between different groups are listed. The D-dimer concentration of unamputated normal mouse plasma was 18 ± 3 ng/ml, which agrees well with the value reported by Castellino and coworkers [75].

Table 1

K_i values for the inhibition of mPm, mXIa and mKLK

Enzyme	K_i Values (nM)[a]		
	KD1$_{WT}$-V$_T$	**KD1$_{L17R}$-K$_T$**	**BPTI[c]**
hPm[b]	6 ± 0.5	0.9 ± 0.1	0.5 ± 0.1
mPm	18 ± 2	4 ± 0.5	1.5 ± 0.3
hXIa[b]	18 ± 2	NM	346 ± 25
mXIa	21 ± 3	3400 ± 300	20 ± 2
hKLK[b]	25 ± 3	NM	18 ± 2
mKLK	20 ± 3	NM	10 ± 2
Bovine Trypsin	17 ± 2	7 ± 1	0.07 ± 0.01

[a] K_i values represent an average of three independent measurements and were determined using the tight binding equilibrium equation [54]. K_i^* values were corrected [53] for the effect of synthetic substrate used for measuring the active concentration of each enzyme employed. Concentration of mPm used was 3 nM, of bovine trypsin was 2 nM and of mXIa or mKLK was 1 nM.

[b] The K_i values for hPm, hXIa and hKLK for each inhibitor are from reference 34. NM, not measurable upto 10 μM;

[c] BPTI, Bovine pancreatic trypsin inhibitor (aprotinin).